



Published in final edited form as:

Science. 2006 May 26; 312(5777): 1220–1223. doi:10.1126/science.1127883.

CRACM1 Is a Plasma Membrane Protein Essential for Store-Operated Ca^{2+} Entry

M. Vig^{1,*}, C. Peinelt², A. Beck², D. L. Koomoa², D. Rabah¹, M. Koblan-Huberson¹, S. Kraft¹, H. Turner², A. Fleig², R. Penner^{2,*}, and J.-P. Kinet^{1,*}

¹Department of Pathology, Beth Israel Deaconess Medical Center and Harvard Medical School, Boston, MA 02215, USA

²Center for Biomedical Research at The Queen's Medical Center and John A. Burns School of Medicine at the University of Hawaii, Honolulu, HI 96813, USA

Abstract

Store-operated Ca^{2+} entry is mediated by Ca^{2+} release-activated Ca^{2+} (CRAC) channels following Ca^{2+} release from intracellular stores. We performed a genome-wide RNA interference (RNAi) screen in *Drosophila* cells to identify proteins that inhibit store-operated Ca^{2+} influx. A secondary patch-clamp screen identified CRACM1 and CRACM2 (CRAC modulators 1 and 2) as modulators of *Drosophila* CRAC currents. We characterized the human ortholog of CRACM1, a plasma membrane-resident protein encoded by gene *FLJ14466*. Although overexpression of CRACM1 did not affect CRAC currents, RNAi-mediated knockdown disrupted its activation. CRACM1 could be the CRAC channel itself, a subunit of it, or a component of the CRAC signaling machinery.

Receptor-mediated signaling in nonexcitable cells, immune cells in particular, involves an initial rise in intracellular Ca^{2+} due to release from the intracellular stores. The resulting depletion of the intracellular stores induces Ca^{2+} entry through the plasma membrane through CRAC channels (1–4). This phenomenon is central to many physiological processes such as T cell proliferation, gene transcription, and cytokine release (3, 5–7). Biophysically, CRAC currents have been well characterized (2, 8, 9), but the identity of the CRAC channel itself and the pathway resulting in its activation are still unknown. Recently, STIM1 (for stromal interaction molecule in *Drosophila*) was identified as an essential component of store-operated calcium entry (10, 11). This protein is located in intracellular compartments that likely represent parts of the endoplasmic reticulum (ER). It has a single transmembrane-spanning domain with a C-terminal Ca^{2+} -binding motif that appears to be crucial for its hypothesized function as the ER sensor for luminal Ca^{2+} concentration. When stores become depleted, STIM1 redistributes into distinct structures (punctae) that move toward

*To whom correspondence should be addressed. mvig@bidmc.harvard.edu (M.V.); rpenner@hawaii.edu (R.P.); jkinet@bidmc.harvard.edu (J.-P.K.).

Supporting Online Material

www.sciencemag.org/cgi/content/full/1127883/DC1

Materials and Methods

Figs. S1 and S2

Tables S1 and S2

and accumulate underneath the plasma membrane. Whether or not STIM1 actually incorporates into the plasma membrane is controversial (10, 12, 13). Although STIM1 is required to activate CRAC currents, its presence or even its translocation appears not to be sufficient to mediate CRAC activation, because lymphocytes from patients with severe combined immunodeficiency (SCID) appear to have normal amounts of STIM1 levels and normal function, yet fail to activate CRAC channels (14). This suggests that other molecular components may participate in the store-operated Ca^{2+} entry mechanism.

To identify genes encoding the CRAC channel or other proteins involved in its regulation, we performed a high-throughput, genome-wide RNA interference (RNAi) screen in *Drosophila* S2R+ cells. The effect of knockdown of each of the ~23,000 genes was tested by fluorescence measurements of intracellular Ca^{2+} concentration in 384-well microplates with an automated fluorometric imaging plate reader (FLIPR, Molecular Devices). Changes in $[\text{Ca}^{2+}]_i$ were measured in response to the commonly used SERCA [sarcoplasmic and endoplasmic reticulum calcium adenosine triphosphatase (ATPase)] inhibitor thapsigargin, which causes depletion of Ca^{2+} from intracellular stores. An example of responses from this primary screen is illustrated in Fig. 1A, obtained from microplate no. 60. All 63 plates contained wells in which double-stranded RNA (dsRNA) against *Rho1* served as negative control and dsRNA against *stim1* as positive control. Higher resolution graphs of the real-time $[\text{Ca}^{2+}]_i$ imaging data are shown in Fig. 1, B and C, from cells treated with dsRNA against *Rho1* (mock) and *stim1*, as well as two genes we later identified as CRAC modulators 1 and 2 (CRACM1 and CRACM2). On the basis of inhibitory efficacy relative to positive and negative controls, we identified ~1500 genes that reduced Ca^{2+} influx to varying degrees (table S1). After eliminating numerous genes based on artifactual fluorescence signals or because they represent known housekeeping genes, cell cycle regulators, and so on, we eventually arrived at 27 candidate genes (table S2) that were subsequently evaluated in a secondary screen using single-cell patch-clamp assays.

From the secondary patch-clamp screen, we identified two novel genes that are essential for CRAC channel function, CRACM1 (encoded by *olf186-F* in *Drosophila* and *FLJ14466* in human) and CRACM2 (encoded by *dpr3* in *Drosophila*, with no human ortholog). We measured CRAC currents in *Drosophila* Kc cells after inositol 1,4,5-trisphosphate (IP_3)–mediated depletion of Ca^{2+} from intracellular stores. Both untreated control wild-type cells and cells treated with an irrelevant dsRNA against *Rho1* (mock) responded by rapidly activating a Ca^{2+} current with the time course (Fig. 1D) and inwardly rectifying current-voltage (I/V) relation (Fig. 1E) typical of I_{CRAC} in mammalian (2) and *Drosophila* (15) cell types. In contrast, CRAC currents were essentially abolished in cells treated with dsRNA for CRACM1 and CRACM2. In some of the experiments on CRACM1, we also applied ionomycin (10 μM) extracellularly on top of the 20 μM IP_3 included in the patch pipette to ensure complete store depletion, but this also failed to induce I_{CRAC} (fig. S1C). Similarly, CRAC currents were also absent when passive store depletion was induced by the Ca^{2+} chelator BAPTA [(1,2-bis(*o*-aminophenoxy)ethane-*N,N,N',N'*-tetraacetic acid)] (fig. S1, A and B).

We studied the human ortholog of CRACM1, a 37.7-kD protein encoded by gene *FLJ14466*, to confirm that its function is conserved across species and that it is involved in store-

operated Ca^{2+} entry. We used small interfering RNA (siRNA)-mediated silencing of human CRACM1 in human embryonic kidney cells (HEK293) and human T cells (Jurkat). The selective knockdown of CRACM1 message was confirmed by semiquantitative reverse transcription polymerase chain reaction (RT-PCR) analysis (Fig. 2A). Two different CRACM1-specific siRNA sequences caused a 60 to 70% inhibition of calcium influx in response to thapsigargin-induced store depletion in HEK293 cells (Fig. 2B). Patch-clamp recordings obtained from siRNA-treated cells, responding to intracellular IP_3 perfusion, demonstrated a nearly complete inhibition of CRAC currents (Fig. 2, D and E). In Jurkat cells, siRNA-mediated inhibition of Ca^{2+} influx was close to 20% (Fig. 2C) and not as dramatic as in the HEK293 cells. However, I_{CRAC} in Jurkat cells was effectively reduced by both siRNA sequences (Fig. 2, F and G). The differences in the efficacy of suppressing the changes in $[\text{Ca}^{2+}]_i$ in HEK293 and Jurkat cells (see Fig. 2, B and C) are likely due to the different magnitudes of I_{CRAC} in these two cell types. CRAC current densities in HEK293 cells (~0.5 pA/pF) are much smaller than typically seen in Jurkat cells (~2.5 pA/pF), and a further inhibition may explain the more dramatic reduction in the Ca^{2+} signal than that observed in Jurkat cells (note that the remaining CRAC current densities in siRNA-treated Jurkat cells, while strongly reduced, are ~0.4 pA/pF and comparable to the normal CRAC current densities of untreated HEK293 cells). Taken together, these data indicate that CRACM1 is also a key modulator of store-operated CRAC currents in human cells.

Given that the knockdown of CRACM1 inhibited CRAC activation, we wanted to know whether overexpression would enhance Ca^{2+} influx and CRAC current densities. HEK293, Jurkat, and RBL-2H3 cells were infected with a Myc-tagged CRACM1 and green fluorescent protein (GFP) retrovirus, and overexpression of the protein was confirmed in HEK293 cells by immunoprecipitation followed by Western blotting (Fig. 3A). However, we did not detect any increase in CRAC current amplitudes above control levels in either HEK293 (Fig. 3B) or Jurkat cells (fig. S2A) and only a slight increase in RBL cells (fig. S2B). These data suggest that CRACM1, although necessary for CRAC activation, does not in and of itself generate significantly larger CRAC currents.

An important question is whether CRACM1 localizes to the ER (as does STIM1) or to the plasma membrane. To address this question, we tagged CRACM1 on either end (Myc-C terminus and flag-N terminus) and transfected the constructs into HEK293 cells. After 24 hours, immunofluorescence confocal analysis revealed no staining in intact cells expressing either construct, which suggested that both tags are intracellular. After permeabilizing the cells, both constructs were detected by the fluorescent antibody and showed predominant peripheral staining of the plasma membrane (Fig. 3, C and D). These data fit well with the hydropathy profile of CRACM1, which predicts a topology of four transmembrane domains, with both ends facing the cytosol (fig. S2C).

In summary, our results demonstrate that the protein CRACM1 is essential for store-operated Ca^{2+} influx via CRAC channels. Although the overexpression of CRACM1 does not alter the magnitude of CRAC currents, the plasma membrane localization of this protein and the presence of multiple transmembrane domains point toward a direct role for CRACM1 in store-operated calcium influx. A number of possible functions can be envisioned for CRACM1. First, CRACM1 could function as the CRAC channel itself. In this scenario, the

unaltered CRAC currents in CRACM1 overexpressing cells might be due to a limiting factor upstream of CRAC channel activation (e.g., STIM1). Second, CRACM1 could be a subunit of a multimeric channel complex, in which case the other subunit(s) could become the limiting factor(s) during overexpression. Finally, CRACM1 might function as a plasma membrane acceptor or docking protein, possibly for STIM1 or some other as-yet-unidentified component of the signaling machinery that ultimately leads to CRAC channel activation and store-operated Ca^{2+} entry.

Supplementary Material

Refer to Web version on PubMed Central for supplementary material.

Acknowledgments

We thank B. Mathey-Prevot, N. Ramadan, M. Booker, and staff at the *Drosophila* RNAi Screening Center at Harvard Medical School for assistance with the screen; V. Yu and M. Xie (Synta Pharmaceuticals, Lexington, MA) for help with using FLIPR; M. Bellinger for help with cell culture; and A. Dani for stimulating discussions and help with imaging experiments. Supported in part by NIH grants 5-R37-GM053950 (J.P.K.), R01-AI050200 and R01-NS040927 (R.P.), R01-GM065360 (A.F.).

References

1. Putney JW Jr. Cell Calcium. 1990; 11:611. [PubMed: 1965707]
2. Hoth M, Penner R. Nature. 1992; 355:353. [PubMed: 1309940]
3. Parekh AB, Penner R. Physiol. Rev. 1997; 77:901. [PubMed: 9354808]
4. Parekh AB, Putney JW Jr. Physiol. Rev. 2005; 85:757. [PubMed: 15788710]
5. Partiseti M, et al. J. Biol. Chem. 1994; 269:32327. [PubMed: 7798233]
6. Lewis RS. Annu. Rev. Immunol. 2001; 19:497. [PubMed: 11244045]
7. Winslow MM, Neilson JR, Crabtree GR. Curr. Opin. Immunol. 2003; 15:299. [PubMed: 12787755]
8. Hoth M, Penner R. J. Physiol. 1993; 465:359. [PubMed: 8229840]
9. Zweifach A, Lewis RS. Proc. Natl. Acad. Sci. U.S.A. 1993; 90:6295. [PubMed: 8392195]
10. Liou J, et al. Curr. Biol. 2005; 15:1235. [PubMed: 16005298]
11. Roos J, et al. J. Cell Biol. 2005; 169:435. [PubMed: 15866891]
12. Zhang SL, et al. Nature. 2005; 437:902. [PubMed: 16208375]
13. Spassova MA, et al. Proc. Natl. Acad. Sci. U.S.A. 2006; 103:4040. [PubMed: 16537481]
14. Feske S, Prakriya M, Rao A, Lewis RS. J. Exp. Med. 2005; 202:651. [PubMed: 16147976]
15. Yeromin AV, Roos J, Stauderman KA, Cahalan MD. J. Gen. Physiol. 2004; 123:167. [PubMed: 14744989]

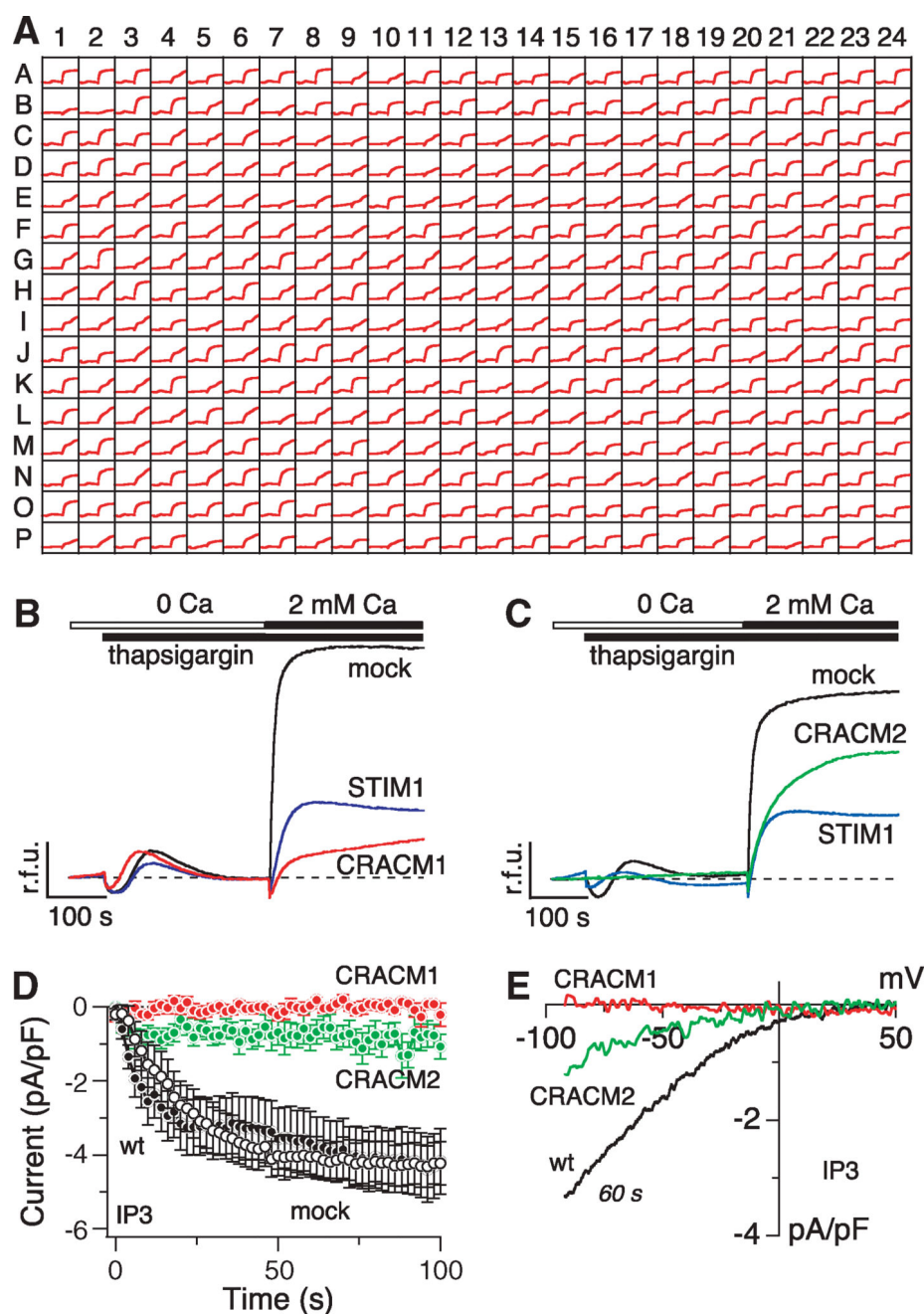
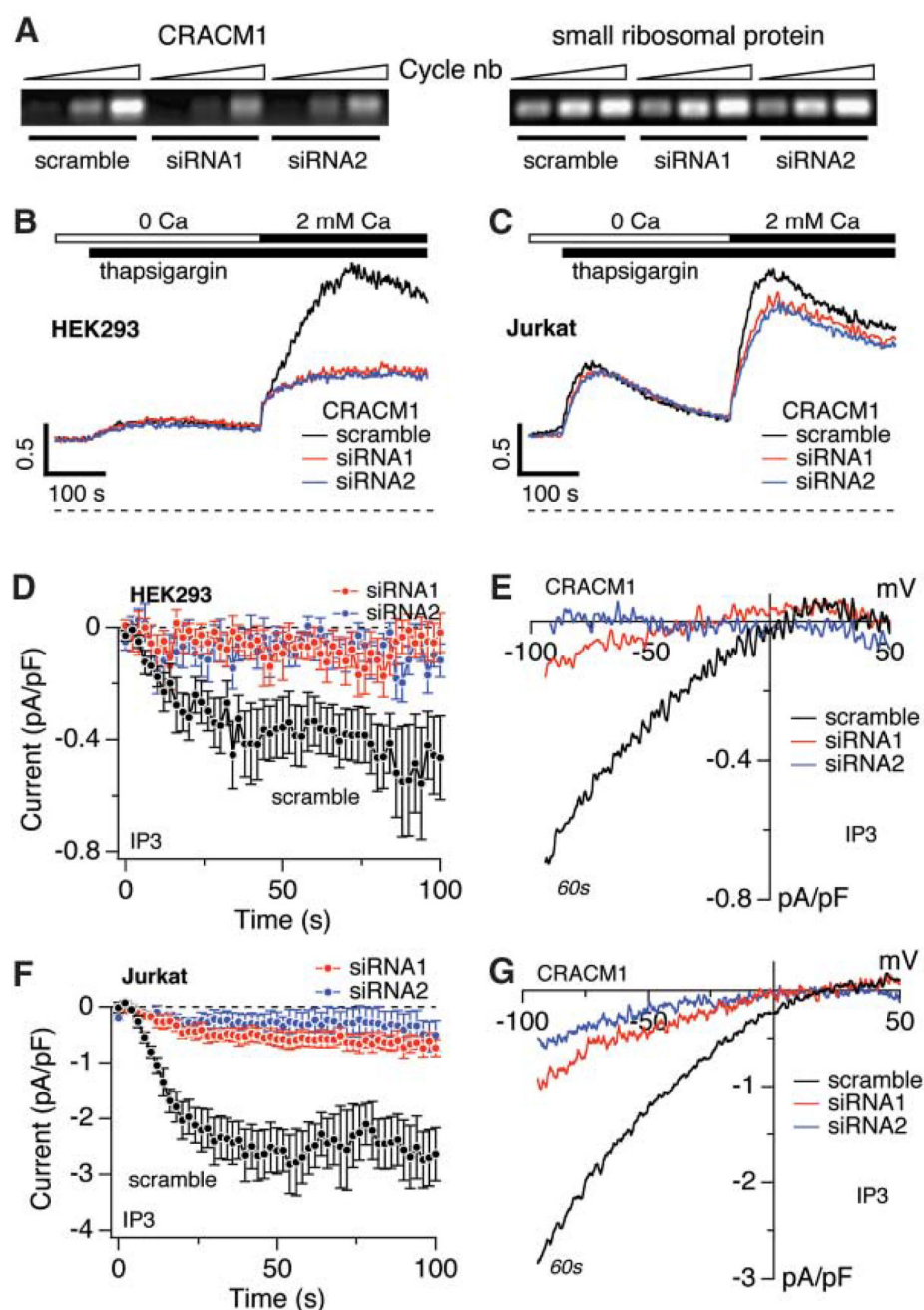


Fig. 1. Identification of CRACM1 and CRACM2 as crucial regulators of store-operated Ca^{2+} entry in *Drosophila*. **(A)** Ca^{2+} signals measured in *Drosophila* S2R+ cells in the primary high-throughput screen using FLIPR. Representative FLIPR raw data file showing 384 minigraphs, each of which represents fluo-4 fluorescence change in an individual well with respect to time. Each plate contained the negative control dsRNA *Rho1* in well A1 and the positive control dsRNA *stim1* in well B1. **(B)** Fluo-4 fluorescence changes in relative fluorescence units (r.f.u.) obtained from cells treated with the indicated dsRNAs. Cells were kept in Ca^{2+} -free solution and exposed to thapsigargin (2 μM), followed by addition of 2

mM Ca^{2+} . The traces are representative of two independent repeats of the primary screen. (C) Same protocol as in (B) but for cells treated with CRACM2 dsRNA. (D) Normalized average time course of IP_3 -induced (20 μM) I_{CRAC} measured in *Drosophila* Kc cells. Currents of individual cells were measured at -80 mV, normalized by their respective cell size, averaged and plotted versus time ($\pm\text{SEM}$). Cytosolic calcium was clamped to 150 nM with 10 mM BAPTA and 4 mM CaCl_2 . Traces correspond to untreated control [wild type (wt), black filled circles, $n = 10$]; Rho1 dsRNA (mock, open circles, $n = 8$); CRACM1 dsRNA (red circles, $n = 6$); and CRACM2 dsRNA (green circles, $n = 9$]. (E) Averaged current-voltage (I/V) data traces of I_{CRAC} extracted from representative cells at 60 s for currents evoked by 50-ms voltage ramps from -100 to $+100$ mV with leak currents subtracted and normalized to cell size (pF). Traces correspond to untreated control (wt, $n = 9$); CRACM1 dsRNA ($n = 5$); and CRACM2 dsRNA ($n = 6$).

**Fig. 2.**

Suppression of store-operated Ca^{2+} entry and I_{CRAC} by CRACM1 siRNA. **(A)** (Left) RT-PCR of CRACM1 mRNA from HEK293 cells infected with the indicated CRACM1-specific siRNAs and a scrambled sequence control. (Right) Control with primers specific for small ribosomal protein. **(B)** Fura 2-AM (pentaacetoxymethyl ester) fluorescence measurements of $[\text{Ca}^{2+}]_i$ in cells treated with scramble (control) or the two CRACM1-specific siRNAs in HEK293 cells. Cells were kept in Ca^{2+} -free solution and exposed to thapsigargin (2 μM), followed by addition of 2 mM Ca^{2+} . The traces are representative of three independent experiments. **(C)** Same protocol as in **(B)**, but for Jurkat cells. The traces are averages of

three independent experiments. **(D)** Normalized average time course of IP₃-induced (20 μM) I_{CRAC} measured in HEK293 cells treated with the indicated siRNAs ($n = 9$ to 13 for each group). $[\text{Ca}^{2+}]_i$ was clamped to near zero by 10 mM BAPTA. **(E)** Current-voltage (I/V) data traces of I_{CRAC} from representative cells at 60 s for currents evoked by 50-ms voltage ramps from -100 to $+100$ mV in cells treated with the indicated siRNAs ($n = 7$ to 10). **(F and G)** Same as panel (D) and (E), but for Jurkat cells ($n = 8$ to 9).

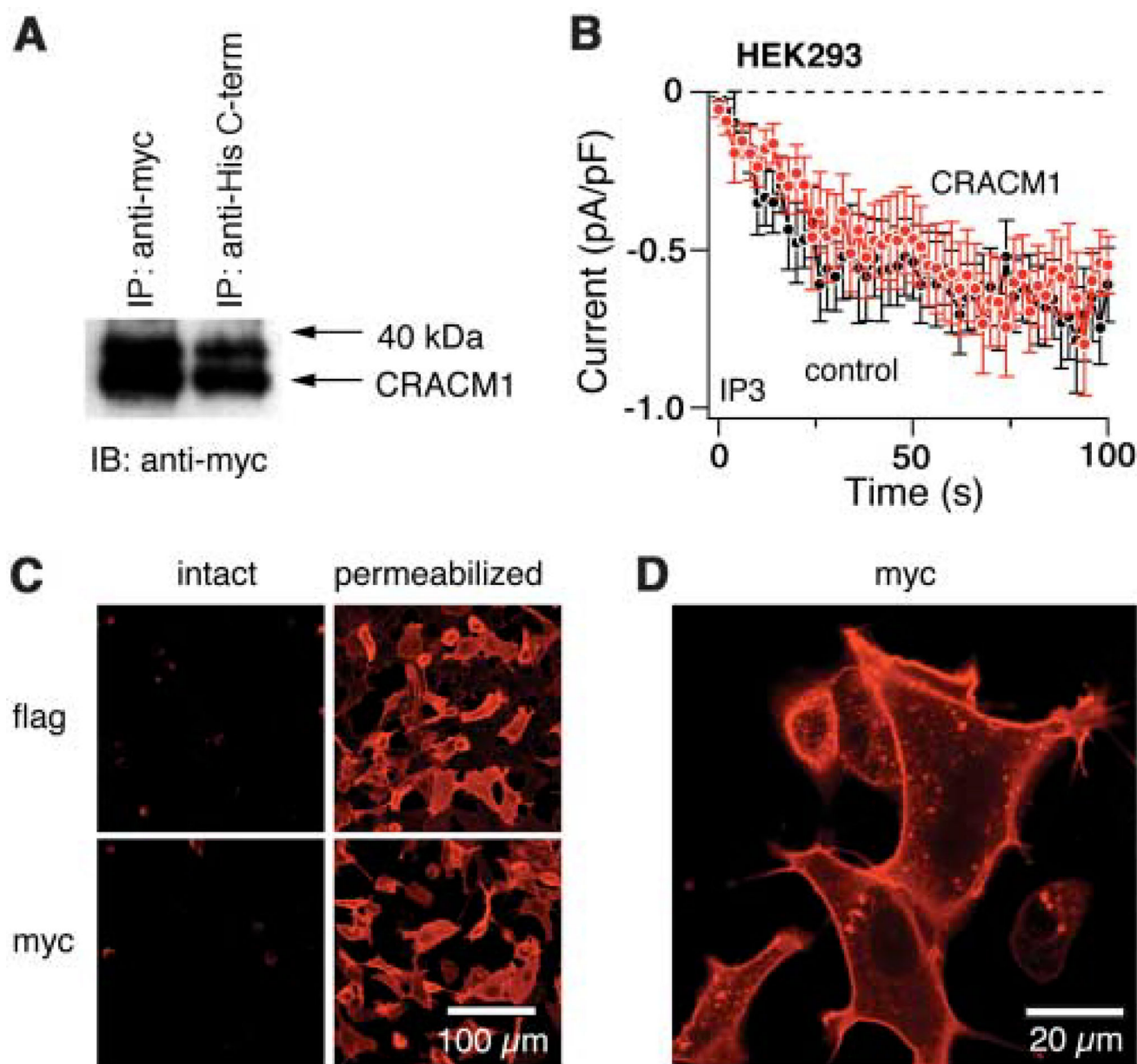


Fig. 3. Overexpression of CRACM1. **(A)** Analysis of HEK293 cells for overexpression of CRACM1 by immunoprecipitation with antibodies against Myc or C-terminal His and immunoblotting with antibody against Myc. Control immunoprecipitation from empty vector-transfected cells did not show any bands. **(B)** Normalized average time course of IP₃-induced (20 μ M) I_{CRAC} measured in HEK293 cells. Currents of individual cells were measured at -80 mV, normalized by their respective cell size, averaged, and plotted against time (\pm SEM). Cytosolic calcium was clamped to near zero by using 10 mM BAPTA. Traces correspond to cells transfected with GFP alone (control, black circles, $n = 13$) and cells transfected with GFP plus CRACM1 (red circles, $n = 14$). **(C)** Immunofluorescence localization of CRACM1 in HEK293 cells visualized by confocal microscopy.

Immunostaining for CRACM1–flag–N terminus (top) or CRACM1–Myc–C terminus (bottom) in intact (left) and permeabilized cells (right). **(D)** Same as bottom right panel of (C), but at higher magnification of selected cells to illustrate plasma membrane staining.

Author Manuscript

Author Manuscript

Author Manuscript

Author Manuscript